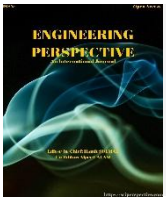

e-ISSN:2757-9077

ENGINEERING PERSPECTIVE

https://sciperspective.com

Research Paper

Thermal Model of Lithium-Ion Batteries for Hybrid Electric Vehicles

Racha Bayzou[1*], Adrien Soloy[1], Thomas Bartoli[1], Fatima Haidar[1]

[1] *Capgemini engineering, Ile de France, Division APA, 12 rue de la Verrerie, 92190 Meudon, France*

ABSTRACT

This study aims to develop a comprehensive model using MATLAB Simulink software to characterize the thermal behavior of lithium-ion battery packs. The model operates at both the cell and pack levels, enabling the determination of individual cell temperatures and the heat generated by Joule effect, influenced by chemical reactions during charge and discharge cycles. At the pack level, the model assesses temperature variations among cells by simulating heat transfers between them. Detailed principles, equations, and underlying hypotheses for constructing the model are elucidated.

Through simulations, the model's performance is evaluated against experimental data. Remarkably, strong correlations are observed in temperature variations of 18650 LFP cylindrical cells within a battery pack, not only under standard charge and discharge conditions but also when subjected to a standardized WLTC (Worldwide harmonized Light vehicles Test Cycle**)** driving cycle. This indicates the robustness and accuracy of the chosen methodology in model development. The study's findings hold significant implications for optimizing battery pack design and advancing thermal management strategies in various applications such as electric vehicles and renewable energy systems.

Future research endeavors may involve further refinement of the model and exploration of additional facets of battery behavior to enhance its predictive capabilities and applicability across diverse scenarios.

Keywords: Hybrid Electric Vehicles (HEV); Li-ion; MATLAB-Simulink; Thermal model.

History
Received: 14.05.2024
Revised : 05.02.2025
Accepted: 03.05.2025

Author Contacts : racha.bayzou@capgemini.com* adrien.soloy@capgemini.com thomas.bartoli@capgemini.com fatima.haidar@capgemini.com

Cite this paper: Bayzou, R., Soloy, A., Bartoli, T., Haidar, F. (2025). Thermal model of Lithium-ion batteries for hybrid electric vehicles. Engineering Perspective, 5 (2), 60-67. http://dx.doi.org/10.29228/eng.pers.76492

*Corresponding Author

1. Introduction

Environmental worries regarding the exhaustion of traditional energy resources have grown on a global scale in recent decades. The signification rise in atmospheric pollution and the greenhouse effect can be largely attributed to the extensive reliance on fossil fuels, particularly in the context of automotive usage [1]. Batteries, particularly Li-ion, have emerged as a solution to replace fossil fuels. While initially costly and offering limited range, Li-ion batteries have undergone substantial advancements in recent years, reducing the cost per kilowatt-hour (kWh) from $1.000 in 2010 to approximately $273 in 2016, with forecasts projecting further reductions to around $109 per kWh by 2025 and $73 per kWh [2-3]. Despite continuous improvements and current energy densities of around 250 Wh/kg, Li-ion batteries still exhibit certain drawbacks [4]. One significant issue is the reliance on metals like lithium and cobalt, which are used in cathode materials such as Lithium Cobalt Oxide (LCO), Nickel Manganese Cobalt (NMC), or Nickel Cobalt Aluminum (NCA) [5]. These materials pose economic challenges due to their uneven geographic distribution and environmental concerns regarding their extraction, which has a substantial environmental impact [6].

Another limitation concerns cell safety in various scenarios such as crushing, puncturing, extreme temperatures, or thermal runaway. Therefore, effective temperature management within the battery pack is crucial. Car manufacturers achieve this through a battery management system (BMS), which incorporates multiples functions like monitoring current, voltage, resistance, state of charge (SOC), state of health (SOH), and thermal conditions within the cells. The BMS communicates with the vehicle's calculator, enabling the regulation of power consumption, the control of the cooling system, and the ability to raise alerts in case of potential dangers.

To address these challenges, the utilization of models to predict the thermal behavior of batteries is a critical concern for both cell and vehicle manufacturers [7-8]. These models help forecast temperature distribution within the cell based on its morphology (e.g., pouch cell, cylindrical, or prismatic cell) and material

composition. They also help to predict the cooling requirements to keep the battery pack in ideal temperature conditions. The cooling demands are influenced by various factors, including the number of cells, their configuration within the battery pack, and the thermal power generated. Proper sizing of these components allows for risk mitigation while optimizing the financial investments required for the development of this strategy. In this context, a straightforward method for predicting the thermal behavior of cells and battery packs is presented in this work. The aim of this study is to create a battery model allowing the simulation of the thermal behavior of cells contained in a Li-ion battery pack and of the battery pack itself. This model is then to be integrated into a complete battery model to be able to study the behavior of Li-ion batteries used in hybrid electric vehicles. The work described here will not detail the integration of the whole battery model but will rather focus on the method used to develop the battery thermal model itself.

2. Model choice consideration

Battery modeling has become essential in the automotive industry for designing high performance hybrid and electric vehicles. By understanding and predicting battery behavior, modeling ensures optimal and safe usage, maximizing performance, lifespan, and efficiency. It enables the development of effective battery management strategies and optimization of design for reliable electric vehicle operation [9] . Depending on the application, battery models vary in complexity, depending on the environment and parameters being analysed. Various types of battery models exist based on the parameters and properties under study. The main battery models found in the literature are: Electrochemical, electrical and thermal [10-11].

Starting the development of a suitable Li-ion battery thermal model, aligned with the predefined technical requirements, required the careful selection of a method. This selection process considered various criteria, including computational cost, simulation time, realism in relation to the physical system, and the complexity of method development and calculations. The following approaches were compared:

-The analytical resolution method for the 2D transient heat equation, employing the Fourier method and separation of variables (transient and steady state). This method incorporates the boundary and initial conditions of the system.

-The finite difference numerical resolution method.

-The finite element numerical resolution method.

-The thermal quadrupole method.

-The series thermal resistance method.

-The matrix method

After an exhaustive bibliographical study analyzing the modeling methods and a comprehensive assessment of different criteria, the matrix method, which is an adaptation of the thermal resistance method, was chosen. This method is not only computationally efficient and straight forward to implement, but it also aligns well with Simulink's matrix calculus constraints for the determination of temperatures and thermal powers.

In the upcoming section, the approach and principles behind the thermal modeling of a cell are detailed, along with the corresponding functionalities that have been developed.

2.1. Thermal model of battery cell

- **Principle**

Before starting the development of the Simulink model, it was imperative to delineate the assorted requirements and technical functionalities that needed to be addressed. Specifically, the Simulink model should allow:

-Compute the temperature of each layer of materials contained within every cell.

-Calculate the heat generated through Joule heating and chemical reactions within the volume of each layer in the cell.

-Facilitate the adjustment of physical parameters via a MATLAB script.

- Enable the modification of the cell dimensions.
- Evaluate thermal exchanges between cells.

-Dynamically compute the heat generated and temperature variations in each layer of every cell.

- **Method**

Initially, various hypotheses and approximations of the physical phenomena of the model were established to simplify the design and validation of the model in Simulink. The case of cylindrical cells was chosen.

The surface temperature is considered homogeneous, the median plane of the cell is mainly studied. Indeed, it is in this plane that the surface temperature is the highest and where temperatures are generally measured using a sensor. In addition, materials through which the conductive flow pass are considered anisotropic. As a result, the conductive flow is oriented in the radial direction (or x, as shown in Figure 1) within cylindrical cells. In addition, contact resistance is neglected. In the center of the cell, the flow is nil because the system under study is symmetrical around its axis. At the outer surface of the cell, the discharged conductive flow is equal to the convective flow. In addition, the initial temperature of the cell is considered the same as that of the fluid in the environment. Eq. (1) and Figure 1 describes and illustrates the boundary conditions of the cell system.

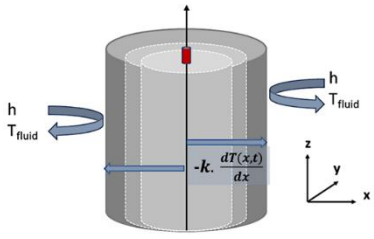

Figure 1. Schematic description of the boundary conditions of the cell.

The development process primarily involved identifying the various stages and requirements of the model. Initial steps included an in-depth examination of diverse thermal modeling techniques applied to Li-ion battery cells, scrutinizing the approach, approximations, and conditions employed. Subsequently, intermediate tests were conducted to validate each functionality of the model as it progressed.

$$\frac{\partial^2 T(r,t)}{\partial r^2} + r.\frac{\partial T(r,z,t)}{\partial r} - \frac{1}{\alpha}.T(r,t) = -\frac{q}{\lambda}$$
$$For\ r = 0, \quad -\lambda \frac{dT(r,p)}{dr} = 0 \qquad (1)$$
$$For = R, \quad -\lambda \frac{dT(r,t)}{dr} = h.\left(T(r,t) - T_{fluid}\right)$$
$$For\ t = 0\ s, \quad T(r,0) = T_{fluid}$$

Table 1. Input and output parameters used for the model.

Input parameters	
Geometric cell properties	
Length	(mm)
Radius	(mm)
Thickness	(mm)
Interlayer exchange area	(mm^2)
Thermophysical properties	
Thermal conductivity	(W/(m.K))
Density	(kg/m^3)
Specific heat capacity	(J/(kg.K))
Boundary conditions properties	
Convective transfer coefficient	($W/(m^2.K)$)
Fluid temperature	(°C)
Convective flux	(W)
Fluid temperature T_{ext}	(°C)
Output parameters	
Surface and core temperatures	(°C)
Layer temperatures	(°C)
Joule effect	(W)
Entropy variation	(W)

These tests played a crucial role in refining and enhancing different versions of the Simulink code in comparison to results obtained from analogous cell models. This iterative process allowed for course correction and improvement, aiding in the selection of an optimal compromise between operational speed and model realism.

Input parameters for the model encompassed geometric, thermophysical data, and boundary conditions such as convective flow, convective transfer coefficient, and outlet temperature. Output parameters included temperatures (core, surface, layers) and various powers generated by the model, such as Joule effect and entropy variation. These parameters are succinctly presented in Table 1.

- **Developed**

After studying and selecting the most suitable method, it became possible to develop various functionalities that meet the initial requirements of the model. Indeed, the Simulink model performs the following:

Calculation of the thermal power generated by current dissipation in the cell through Joule effect and entropy variation is achieved by a Simulink subsystem. This subsystem takes the current of each cell, squares it, and multiplies it by the internal resistance of each cell. The thermal power generated by entropy variation during the electrochemical reaction due to charging or discharging is calculated based on the current of each cell, its open-circuit voltage, and temperature.

Calculation of the fraction of power generated within the volume of each layer. A block takes the total power generated for a cell and multiplies it by a fraction of the volume associated with each layer. This volumetric fraction depends on the thickness of each layer.

Calculation of the temperature of each layer in each cell. It is performed by a MATLAB function integrated into the Simulink code. This function calculates the temperature of the first layer of the cell based on the initial temperature, the cell, the heat generated by the Joule effect, and the exchange surface between the cells. A balance of exchanged flows with the next layer is then conducted. Incoming and outgoing conductive fluxes are considered for internal layers.

Modification of the thermophysical and geometric parameters of the model through the execution of an initialization script. A script corresponding to the chosen cell technology is executed in advance on MATLAB to load different thermophysical and geometric parameters of the cell in the Simulink model. The ability to modify parameters in the script allows us to adapt easily the simulation to various cell technologies.

Calculation of thermal exchanges between cells. It is performed by a MATLAB function that retrieves the calculated temperature in different layers of a cell to extend the calculation to all cells constituting a battery pack.

The sequence of execution of various functionalities and the calculation steps of different quantities in the model are depicted in Figure 2. The main functionalities of the Simulink thermal model that has been developed are presented in Figure 3.

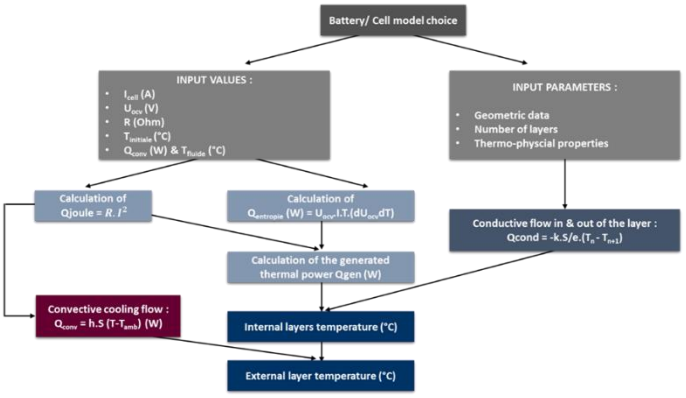

Figure 2. Calculation steps followed by the thermal model developed in Simulink.

It is worth noting that the current model includes certain limitations, such as the assumption of uniform material properties and steady-state operating conditions.

2.2. Thermal model of pack battery

- **Pack model based on the cell model**

The three-layer model describing cell behavior is used to build a comprehensive battery pack model. This section will present the model development process, outline the various assumptions and approximations made, and detail the results obtained.

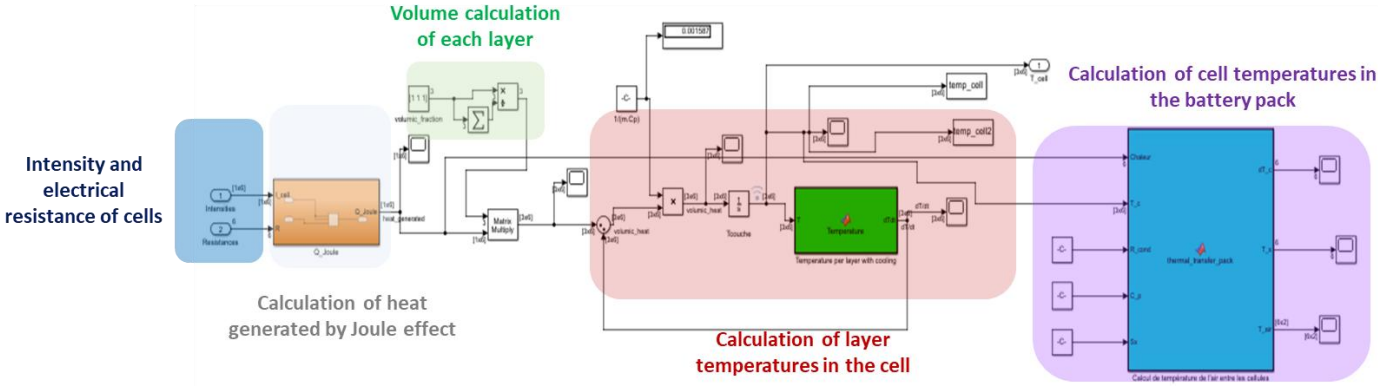

Figure 3. Simulink models and related features

The objective of the model is to simulate heat transfers among the cells constituting a battery pack. As for the Simulink-developed cell model, several assumptions, and approximations regarding the physical phenomena of the model were established to streamline the design and validation of the thermal model for a battery pack:

Cells are assumed to be spaced apart, allowing for fluid flow between them.

Radiative heat losses are disregarded in comparison to those transferred by convection inside the battery pack. Indeed, radiant energy constitutes only a minimal portion of the energy exchanged during cell charging and discharging.

The conductive flow through the foils (metal lamellae) connecting individual cells in series within the battery pack is also neglected.

Incoming air is blown at room temperature, and its flow is evenly distributed among the cells. Heat propagation between cells occurs from left to right and from bottom to top, following the air flow. Consequently, the convective exchange coefficient remains consistent throughout the battery pack.

Heat transfer between cells was analyzed in various scenarios based on each cell's position within the battery pack. These scenarios include:

The cell in the lower-left corner is at the temperature of the incoming air at the beginning of the simulation. The temperatures of other cells are then calculated based on the temperature of the air, the airflow, and the temperature of this first cell.

Cells in the first lower row transfer heat through convection and then conduct in the air to the adjacent cells in the upper row. Because of the proximity of the cells and the low airflow, the convective transfer is neglected.

Cells in the first column on the left transfer heat through convection to the neighboring cells in the next column on the right.

Various convective heat exchange patterns between cells were considered [12]. Cells are arranged in rows in parallel and series. The model extracts the temperature of the first layer calculated by the cell calculation block as a vector. This vector is then put into the cell temperature calculation block to initialize the core, surface, and air temperatures of the cells. Groups of surface, core, and air temperatures are stored in matrices, which size is determined by the number of cells in parallel and in series. This number is set in the initialization script of the simulation. Cells in the vertical direction "i" are in series, while cells in the horizontal direction "j" are in parallel. The temperature calculation method is directly inspired from the finite difference method applied to a transient two-dimensional thermal problem.

Heat transfers from cells located in two adjacent vertical rows are described by Eq. (2):

$$h_{conv}.S.\left(T_s(i,j) - T_{air}(i,j-1)\right) - h_{conv}.S.\left(T_s(i,j) - T_{air}(i,j)\right) - \frac{\lambda.S}{e}.\left(T_c(i,j) - T_s(i,j)\right) = 0 \quad (2)$$

Where S denotes the exchange surface between the cell and the ambient fluid (m²), e is the cell thickness, h_{conv} is the convective exchange coefficient between the cell surface and the ambient air (W/ (m².K)), λ is the thermal conductivity of the cell (W/(m.)), T_s (i,j) is the temperature of the surface of the cell located on the row i and column j, T_{air} (i,j-1) denotes the temperature of the air at the row i and column (j-1), T_{air} (i,j) is the temperature of the air at the row i and column j and T_c (i,j) is the temperature of the core of the cell located at the row i and column j.

Figure 4 illustrates the equivalent circuit used to model the horizontal heat transfers between two adjacent cells. It represents the calculus of the temperature of the cell located on the right adjacent vertical row.

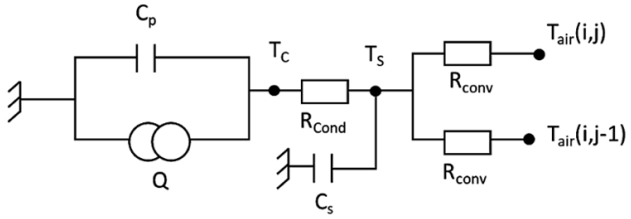

Figure 4. Equivalent circuit represents the horizontal heat transfer between two adjacent cells.

For cells located in the first vertical row, the exchanged thermal power balance between two consecutive cells is expressed by Eq. (3).

$$\text{For } j = 1: \quad \dot{m}_{air}.Cp_{air}.\left(T_{air}(i+1,j) - T_{air}(i,j)\right) = h_{conv}.S.\left(T_s(i,j) - T_{air}(i,j)\right) \quad (3)$$

Where $\dot{m}_{air}$ denotes the air mass flow rate between the cells (kg/s), Cp_{air} represents the air calorific capacity (J/(kg.K)), T_{air} (i+1,j) is the air temperature at the row i+1 and column j, T_{air} (i,j) is the air

temperature at the row i and column j, h_{conv} represents the convective exchange coefficient between the cell surface and the ambient air (W/(m².K)), S is the exchange surface between the cell and the ambient fluid (m²), T_s (i,j) denotes the temperature of the surface of the cell located on the row i and column j and T_{air} (i,j) is the temperature of the air at the row i and column j.

For cells located in the last vertical row, the exchanged thermal power balance between two consecutive cells is expressed by Eq. (4) :

$$\text{For } j = n_p: \quad \dot{m}_{air}.Cp_{air}.\left(T_{air}(i+1,j) - T_{air}(i,j)\right) = h_{conv}.S.\left(T_s(i,j-1) - T_{air}(i,j)\right) \tag{4}$$

Where n_p denotes the number of cells in parallel, $\dot{m}_{air}$ is the air mass flow rate between the cells (kg/s), Cp_{air} is the air calorific capacity (J/(kg.K)), T_{air} (i+1,j) denotes the air temperature at the row i+1 and column j, T_{air} (i,j)is the air temperature at the row i and column j, h_{conv} present the convective exchange coefficient between the cell surface and the ambient air (W/(m².K)), S is the exchange surface between the cell and the ambient fluid (m²), T_s (i,j-1) is the temperature of the surface of the cell located on the row i and column j-1 and T_{air} (i,j) is the temperature of the air at the row i and column j.

For cells located between the first and the last vertical row, the exchanged thermal power balance between two consecutive cells is expressed by Eq. (5).

$$For\ j \in (2, n_p - 1): \quad \dot{m}_{air}.Cp_{air}.\left(T_{air}(i+1,j) - T_{air}(i,j)\right) = h_{conv}.S.\left(T_s(i,j-1) - T_{air}(i,j)\right) + h_{conv}.S.\left(T_s(i,j) - T_{air}(i,j)\right) \tag{5}$$

Where n_p denotes the number of cells in parallel, $\dot{m}_{air}$ is the air mass flow rate between the cells (kg/s), Cp_{air} is the air calorific capacity (J/(kg.K), T_{air} (i+1,j)present the air temperature at the row i+1 and column j, T_{air} (i,j)is the air temperature at the row i and column j, h_conv correspond to the convective exchange coefficient between the cell surface and the ambient air (W/(m².K)), S is the exchange surface between the cell and the ambient fluid (m²), T_s (i,j) present the temperature of the surface of the cell located on the row i and column j and T_{air} (i,j) is the temperature of the air at the row i and column j.

Figure 5 illustrates the process for computing the temperature of cells in the first vertical row. The arrangement of cells and the different heat transfers within the battery pack are illustrated in Figure 6.

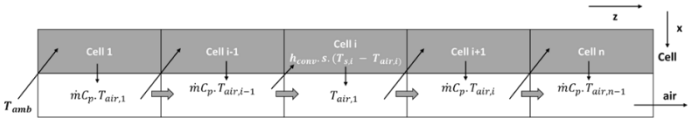

Figure 5. Representation of the heat transfers distribution between the cells of the first vertical row.

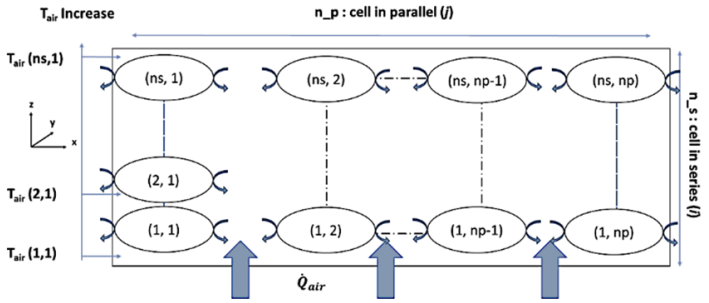

Figure 6. Representation of the heat transfers distribution between the cells of a battery pack.

3. Results and discussion

- **Simulation results at the cell level:**

Tests were first performed at the cell level to check the relevance of the model using characteristics of cells often used in HEV batteries. The parameters of the cylindrical cell chosen for the tests are detailed in Table 2. A comparison was performed between the results obtained experimentally in D. Allart's thesis work [13] and those derived from the Simulink model for charge and discharge currents, presented in the form of analogous squared signals at the model's input. The results are presented in Figure 7. The profile of the surface and core temperature curve for the Simulink model closely resembles that of Allart's thesis [13]. In our model, the surface temperature reaches its maximum at 42 °C, while a value of 43 °C is reported in the thesis. This difference can be attributed to the fact that the heat capacity of the cell is estimated to be 3 layers in the Simulink model, whereas it is estimated for only one layer in the thesis model. As a result, the mass of each layer differs slightly from that used for the cell in the thesis. Another potential explanation for this temperature difference could be the overestimation of the convection exchange surface between the cell and the ambient air in our model compared to the value provided in the thesis.

Another test was performed with currents obtained from a WLTC driving cycle used as input. The aim was to check if the values of temperature increases obtained for one cell were consistent with the literature [12, 14]. The WLTC on which tests are based is presented in Figure 9.

Table 2. Parameters of an 18650 LFP cylindrical cell used for validation tests.

Geometrical parameters	
Number of layers	3
Thickness (mm)	0.0045
Radius (m)	0.009
Mass (kg)	0.0128
Electrical parameters	
Current intensity (A)	3.6
Internal resistance (Ohm)	0.004
Thermophysical parameters	
Thermal conductivity (W/m.K)	0.65
Heat capacity (J/kg/K)	1280
Convective transfer coefficient (m².K)	20
Fluid temperature (°C)	20

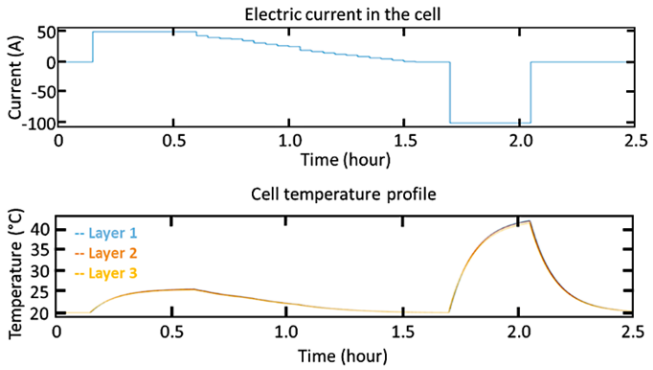

Figure 7. Results obtained by the Simulink model for a 18650 LFP cylindrical cell.

Throughout the vehicle's acceleration phases, the power generated and supplied by the battery rises as the battery discharges. Similarly, the power generated and recovered by the battery increases as its current load escalates during deceleration phases. The curves depicted in Figure 9 illustrate the temperature increase in a cylindrical cell and the fluctuations in current and generated power corresponding to the WLTC cycle used and illustrated in Figure 8.

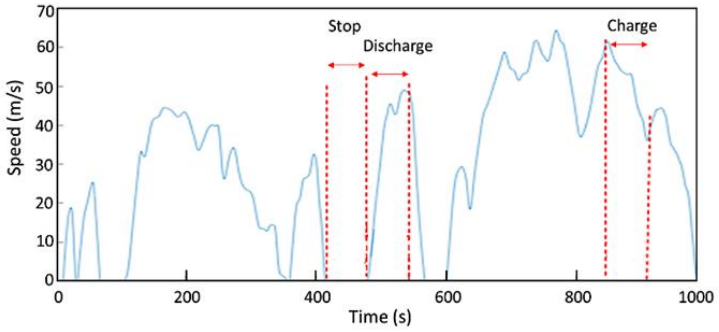

Figure 8. Speed curve of a 1000 second WLTC driving cycle.

The temperature increase remains below 3 °C for a convection coefficient of 10 W/(m²·K) and a power of up to 40 W per cell. These temperature rises are consistent with experimental data documented in the literature for this cell type under similar power and test conditions [13]. Furthermore, it is observed that during vehicle acceleration or deceleration, the cell internal temperature increases because of the current flowing through the layers, heating up the cells. When the vehicle is stopped, with no power required and generated by the battery, the cell temperature decreases due to convection at its surface. The results obtained are consistent and realistic, capturing the physical phenomena experienced by the cells.

The results obtained from the previous test allowed us to visualize the one-dimensional temperature evolution within the various layers of the cell, as shown in Figure 10. The temperature of the first layer, corresponding to the core of the cell, is higher than that of the other layers. This is because the central region of the cell retains heat for a longer duration, requiring successive transfers between the layers before dissipating the accumulated heat through convective flow to the outer layers.

Another test was to compare the results from the Simulink model with those of another model using the "Simscape" library, which incorporates pre-implemented physical and thermal computational functions.

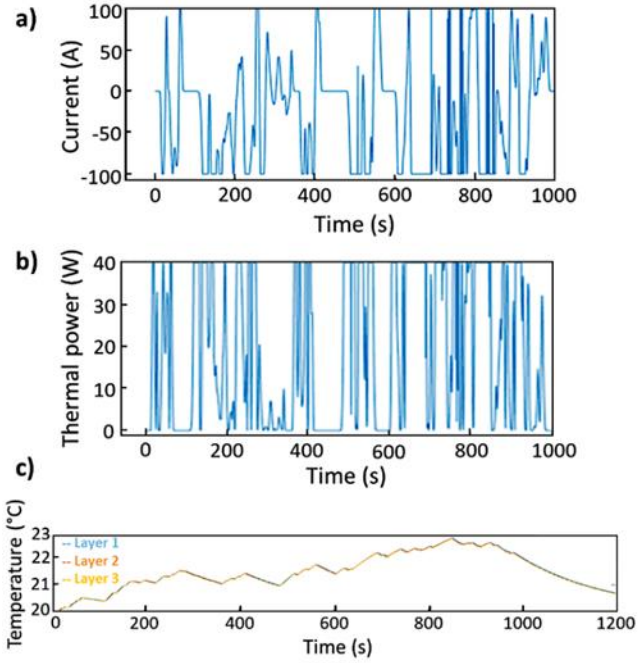

Figure 9. Simulink model results for a WLTC cycle: electric current in the cell (a), thermal power generated in the cell (b) and cell temperature profile (c).

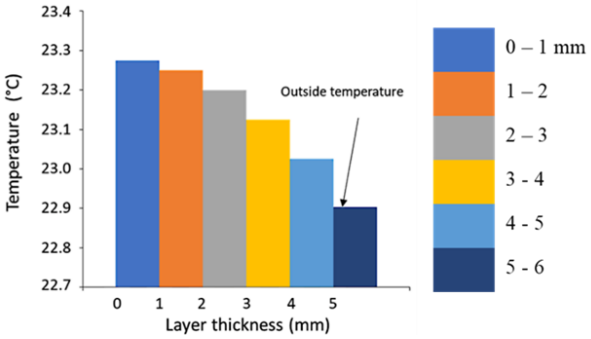

Figure 10. Cell temperature evolution within a cell.

The input conditions and parameters for both models were identical. The objective of this test was to observe the impact of parameters and equations used in the Simulink model to achieve similar results with the Simscape model. The test was conducted at an ambient temperature of 0 °C and a convective flux of 15 W/(m²·K). Initial physical parameters used in both models were the same based on values provided in Table 2. The temperature profiles obtained for the two models are depicted in Figure 11. Similar temperature rises of 2.2 °C and 1.7 °C were observed for the Simulink and the Simscape model of a three-layer cell respectively. The temperature difference between the two models may be attributed to the distinct calculation method used for the convective heat dissipation. The approximations made in the Simulink model, as well as the unknown approximations in the Simscape model, could also account for this temperature difference. The absence of accessible details regarding the approximations made by the Simscape model prevents conclusive remarks on this matter. Both models had identical input conditions, currents, and thermophysical parameters for the cell layers. These tests thus provided an alternative means of validating the

coherence and reliability of the Simulink model.

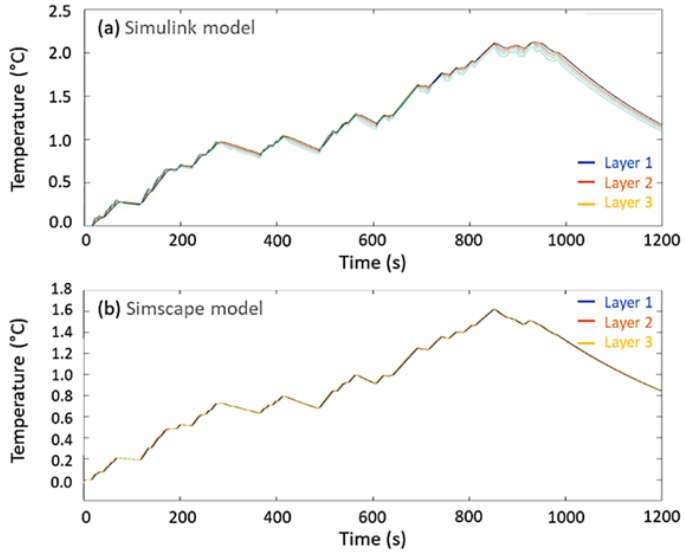

Figure 11. Temperature profiles obtained with the Simulink (a) and the Simscape models (b).

- **Simulation results at the battery pack level:**

Like for the cell model, validation tests were conducted to ensure the physical coherence of the model's behavior at the battery pack level. These tests primarily focused on examining the core and air temperature profiles of LFP cylindrical cells. The cell temperature values were derived from the temperature calculation carried out for a single cell. Consequently, the core temperature of the initial cell allowed the calculation of the core, surface, and ambient air temperatures for the remaining cells. The parameters used for the validation tests for the battery model are shown in Table 3.

Table 3. Parameters of 18650 LFP cylindrical cell used in the battery pack model for validation tests.

Cell thermophysical parameters	
Number of cells	12
Thermal conductivity (W/m/K)	0.65
Radius (m)	0.009
Mass (kg)	0.0128
Internal resistance (Ohm)	0.004
Air thermophysical parameters	
Air density (kg/m^3)	1.225
Air mass flow (kg/s)	0.001
Heat capacity (J/kg/K)	1004
Convective transfer coefficient (W/m^2.K)	5
Fluid temperature (°C)	20

Figure 13 illustrates the variations in surface and air temperature surrounding the cells in a battery pack comprising four rows in parallel and three rows in series. It can be observed that the air temperature surrounding each cell is marginally lower than the surface temperature of the cells. This discrepancy is attributed to the transient mode during which the dissipated heat flow relies on a temperature difference, resulting in the cell surface being warmer than the air. Consequently, four distinct groups of air temperature, corresponding to the heating of the air between the four rows of cells in series, can be identified. The model effectively accounts for the heating of the air along the parallel rows. Conversely, cells situated farthest from the air inlet exhibit the highest temperatures, with the air temperature in the first row being at room temperature (20 °C). These outcomes are aligned with physical realities and are consistent with similar experimental models documented in the literature [12, 14-15], thus reflecting that the model is functional.

4. Conclusions

In this paper, the method used to conceive an accurate lithium-ion battery model is provided. This model comprises a simulation of the heat generated within a single battery cell, each cell being represented by a three-layer stacking, as well as the heat transfers occurring between the cells contained in a battery pack subjected to multiple consecutive charge and discharge cycles. Using heat transfer equations and equivalent circuit models, the thermal behaviour of a battery pack and each of its individual cells is modelled accurately. Simulations were carried out and compared to experimental data available in the literature. The results obtained from the model have shown good correlation with those data. The model built in this work accurately simulates the temperature evolution within an individual cell and the heat transfers in a battery pack. At the cell level, the heat generation modelled was very close to the one illustrated in the literature, both following a single charge-discharge cycle and the different charge-discharge cycles generated by a WLTC standardized driving cycle. The evolution of the temperature of the cell, from the core to the surface, was consistent with experimental observations. The comparison between the Simulink model built in this work and a Simscape model built from pre-implemented physical and thermal computational functions was another proof of the relevancy and accuracy of the model. At the battery pack level, the method heat transfers between the cells, showing consistent heat propagation between the different rows of the pack in series and in parallel. To improve the model further, several works will be carried out in the future such as implementing the failure cases and their consequent thermal runways, considering the thermal losses by radiations, or comparing the simulation results with experimental data for other cell chemistries (NMC, NCA, …).

An additional validation step involved comparing the results obtained from the Simulink model with those generated by an alternative model built using the Simscape library, which includes pre-configured physical and thermal computation components**.**

In the end, this model will be implemented in a complete battery simulation platform aiming to accurately model the electrical, thermal, and ageing behavior of a battery.

Acknowledgment

This work was carried out at Altran Prototypes Automobiles (APA) as a part of the Intelligence & Innovation Powertrain (IPWT) project within the Capgemini Engineering Research and Innovation Department. The authors would like to thank Dr. Mohand-Ouyahia BOUSSEKSOU and Thomas Lozac'h for their contributions to the work.

Conflict of Interest Statement

All authors have given approval to the final version of the manuscript. The authors declare that there is no conflict of interest in the study.

CRediT Author Statement

Racha Bayzou: Writing original draft - review & editing & validation.
Adrien Soloy: Writing original draft & editing.
Thomas Bartoli: Writing original draft, Data collection; Simulation & validation.
Fatima Haidar: Writing original draft & editing.

References

1. Tsolakis, A., Bogarra, M., & Herreros, J. (2017). Road vehicle technologies and fuels. In Environmental Impacts of Road Vehicles: Past, Present and Future (pp. 1–24). Royal Society of Chemistry. https://doi.org/10.1039/9781788010221-00001
2. Ziegler, M. S., & Trancik, J. E. (2021). Re-examining rates of lithium-ion battery technology improvement and cost decline. Energy & Environmental Science, 14(4), 1635–1651. https://doi.org/10.1039/D0EE02681F
3. Ziegler, M. S., Song, J., & Trancik, J. E. (2021). Determinants of lithium-ion battery technology cost decline. Energy & Environmental Science, 14(12), 6074–6091. https://doi.org/10.1039/D1EE01313K
4. Łukasz, B., Rybakowska, I., Krakowiak, A., Gregorczyk, M., & Waldman, W. (2023). Lithium batteries safety, wider perspective. International Journal of Occupational Medicine and Environmental Health, 36(1), 3–20. https://doi.org/10.13075/ijomeh.1896.01995
5. Tran, M. K., DaCosta, A., Mevawalla, A., Panchal, S., & Fowler, M. (2021). Comparative study of equivalent circuit models performance in four common lithium-ion batteries: LFP, NMC, LMO, NCA. Batteries, 7(3), 51. https://doi.org/10.3390/batteries7030051
6. Lèbre, É., Stringer, M., Svobodova, K., Owen, J. R., Kemp, D., Côte, C., Arratia-Solar, A., & Valenta, R. K. (2020). The social and environmental complexities of extracting energy transition metals. Nature Communications, 11, 4823. https://doi.org/10.1038/s41467-020-18661-9
7. Soloy, A., Bartoli, T., & Haidar, F. (2023). Modelling and fault diagnosis of lithium-ion battery for electric powertrain. International Journal of Automotive Science and Technology, 7(3), 234–247. https://doi.org/10.30939/ijastech..1295130
8. Haidar, F., Arora, D., Soloy, A., & Bartoli, T. (2024). Membrane Fuel Cell Degradation and its Counter Strategies: Flooding/drying, Cold Start and Carbon Monoxide Poisoning. *International Journal of Automotive Science and Technology*, 8(1), 96–109. https://doi.org/10.30939/ijastech..1389241
9. Blondel, P. (2019). *Estimation de l'état interne d'une batterie lithium-ion à l'aide d'un modèle électrochimique* (Doctoral dissertation, Université de Lorraine). https://hal.univ-lorraine.fr/tel-02096451
10. Camas-Náfate, M., Coronado-Mendoza, A., Vega-Gómez, C. J., & Espinosa-Moreno, F. (2022). Modeling and Simulation of a Commercial Lithium-Ion Battery with Charge Cycle Predictions. *Sustainability*, 14(21), 14035. https://doi.org/10.3390/su142114035
11. Neverova, N., Wolf, C., Lacey, G., Fridman, L., Chandra, D., Barbello, B., & Taylor, G. (2016). Learning human identity from motion patterns. *IEEE Access*, *4*, 1810–1820. https://doi.org/10.1109/ACCESS.2016.2633260
12. Y. Jannot, *Theory and practice of thermal metrology*, Nancy, France: LEMTA, University of Lorraine, 2011.
13. Allart, D. (2018). Electrothermal management and modeling of lithium-ion batteries [Doctoral dissertation, University of Caen Normandy].
14. Hémery, C.-V. (2014). Study of thermal phenomena in Li-ion batteries [Doctoral dissertation, Université Grenoble Alpes].
15. Guingane, T. T., Bonkoungou, D., Korsaga, E., Simpore, D., Ouedraogo, S., Koalaga, Z., & Zougmore, F. (2023). Evaluation of the performance of lithium-ion accumulators for photovoltaic energy storage. *Energy and Power Engineering*, *15*, 517–526. https://doi.org/10.4236/epe.2023.1512029